Available online at www.sciencedirect.com
ScienceDirect
Colloids and Surfaces A: Physicochem. Eng. Aspects 313–314 (2008) 150–153
COLLOIDS AND SURFACES A
www.elsevier.com/locate/colsurfa

Biomimetic coating of gold nanoparticles with ultrathin silica layers

Sung Min Kang [a], Bang Sook Lee [b], Sang-gi Lee [b,**], Insung S. Choi [a,*]

[a] *Department of Chemistry and School of Molecular Science (BK21), Center for Molecular Design and Synthesis, KAIST, Daejeon 305-701, Korea*
[b] *Division of Nano Science (BK 21) and Department of Chemistry, Ewha Womans University, Seoul 120-750, Korea*

Received 10 October 2006; accepted 23 April 2007
Available online 31 May 2007

Abstract

Encapsulation of nanoparticles has attracted a great attention as a method for stabilizing nanoparticles and subsequently applying them to various areas of technologies. Especially, the encapsulation of nanoparticles with silica shells has proven advantageous for applications to (nano)biotechnology with the well-established silica chemistry. However, current chemical approaches to the formation of silica shells generally require harsh conditions. In contrast, biological processes are capable of generating silica nano/microstructures under ambient conditions. In this work, we formed ultrathin (∼1.5 nm) silica shell-coated nanomaterials by mimicking the biological processes. The procedure consists of simple two steps: immobilization of a thiol-terminated imidazolium ion onto gold nanoparticles (AuNPs) and biomimetic polycondensation of silicic acids. The resulting AuNP/silica hybrids were characterized by Fourier-transform infrared spectroscopy, transmission electron microscopy, and UV–vis spectroscopy.

Keywords: Biosilicification; Gold nanoparticle; Silica shell

1. Introduction

The interest in biomineralization – the deposition of inorganic materials by organisms – has increased enormously because of the facile and mild synthesis of inorganic materials in a controlled manner compared with the chemical synthesis of inorganic materials that generally requires harsh conditions. Particularly, biosilicification (silica biomineralization), found in diatoms [1] and glass sponges [2], has been of interest in nanotechnology and materials sciences [3] because it occurs under ambient conditions at slightly acidic pH values and the formed silica structures are precisely controlled at the nanometer scales. For example, the biosilicification in diatoms is achieved by specific interactions between silicic acid derivatives and biopolymers, such as cationic polypeptides named silaffins containing long-chain polyamines [4]. With the aim of fabricating custom-tailored nanostructures based on the biosilicification, silica nanospheres have been produced *in vitro* with various polyamines, such as poly-L-lysine [5], poly(allylamine hydrochloride) [6], amine-terminated dendrimers (PPI and PAMAM) [7], and others [8]. In addition to the silica nanospheres, the metal/silica core/shell hybrids also have attracted a great deal of attention in the materials sciences and nanotechnology. Because chemistry of silica surfaces is well established, silica-based encapsulation of metal nanoparticles would make it possible to achieve various post-functionalizations of the resulting nanostructures, such as bioconjugation, for the advanced use of metal nanoparticles [9].

Silaffins are post-translationally modified peptides where many of the lysines are modified to ε-*N*-dimethyllysine or oligo-*N*-methylpropyleneimine-linked lysine [4]. Based on the fact that the long-chain polyamines and other amines found in the silaffins are mostly methylated tertiary amines, we have utilized poly(2-(dimethylamino)ethyl methacrylate) (*p*DMAEMA) to biomimetically generate silica structures, such as thin films [10] and micropatterns [11]. More recently, we also could control the thickness of silica layers on gold nanoparticles (AuNPs) by combining surface-initiated atom transfer radical polymerization (SI-ATRP) and biosilicification, in which the thickness of silica layers was critically dictated by the thickness of *p*DMAEMA

* Corresponding author. Tel.: +82 42 869 2840; fax: +82 42 869 2810.
** Corresponding author. Tel.: +82 2 3277 4505; fax: +82 2 3277 3419.
E-mail addresses: sanggi@ewha.ac.kr (S.-g. Lee), ischoi@kaist.ac.kr (I.S. Choi).

0927-7757/$ – see front matter © 2007 Elsevier B.V. All rights reserved.
doi:10.1016/j.colsurfa.2007.04.085

layers [12]. However, the employed procedure composed of the formation of self-assembled monolayers, SI-ATRP, and silicification, was not practically simple but time demanding, although it had an advantage of thickness control. In this study, we formed an ultrathin silica shell on AuNPs by simpler method. Specifically, we chose a thiol-terminated imidazolium ion as a synthetic counterpart of silaffins for silica biomineralization. Thiol-terminated imidazolium ion forms self-assembled monolayers (SAMs) on the surface of AuNPs due to the interaction between thiol and gold, with the imidazolium moiety present at the exterior. We reasoned that the positively charged imidazolium group also would catalyze the biomimetic silicification because our previous result showed that the positively charged, quaternized *p*DMAEMA catalyzed the silicification [13]. In addition, we anticipated that we could form ultrathin silica layers by using the imidazolium ion-presenting SAM, because the biosilicification occurs along organic templates [3,12].

2. Experiment

2.1. Materials

Hydrogen tetrachloroaurate trihydrate ($HAuCl_4 \cdot 3H_2O$, Aldrich), sodium citrate dihydrate (Na_3citrate$\cdot 2H_2O$, 99%, Aldrich), ethanol (99.9%, Merck), tetramethyl orthosilicate (TMOS, >99%, Aldrich), sodium phosphate monobasic (99%, Sigma), sodium phosphate dibasic (99%, Sigma) were used as received. The thiol-terminated imidazolium ion, 1-methyl-3-(12-mercaptododecyl)imidazolium bromide, was prepared according to our reported procedure [14].

2.2. Synthesis of AuNPs and formation of imidazolium ion-presenting SAMs on the surface of AuNPs

AuNPs were synthesized according to the reported procedures [15]. To an aqueous solution (50 mL) of 0.01% (w/v) $HAuCl_4$ that was at a boil, an aqueous solution (1.75 mL) of 1% (w/v) Na_3citrate was added. The resulting mixture was refluxed for 5 min and allowed to cool to room temperature. The color of the solution was changed from grey to red through lavender.

The aqueous solution of imidazolium ion (1 mM, 0.25 mL) was mixed with the AuNP solution (3 nM, 1 mL) at room temperature, and the mixture was incubated overnight. Imidazolium ion-immobilized AuNPs were collected by centrifuge and dispersed in HCl solution (10 mM). The resulting AuNPs were finally washed with sodium phosphate buffer (1 mM, pH 6) several times.

2.3. Formation of AuNP/silica core/shell hybrid structures

For the formation of AuNP/silica hybrids, the resulting imidazolium ion-immobilized AuNPs were dispersed in phosphate buffer solution (1 mM, pH 6, 0.5 mL) (Solution A). Monosilicic acid was independently formed by stirring an HCl solution (1 mM) of TMOS (100 mM) at room temperature for 15 min, and 0.5 mL of the resulting solution was added to 0.5 mL of Solution A. After 1 h, AuNP/silica hybrids were separated from the suspension by centrifugation and washed several times with water by repeated centrifuging/redispersing.

2.4. Characterizations

FT-IR spectra were recorded using NEXUS (ThermoNicolet) and UV–vis spectroscopic measurement was performed on a UV-2550 spectrophotometer (Shimadzu). Transmission electron microscopy (TEM) images were obtained with EM912 Omega (Carl Zeiss) and energy-dispersive X-ray (EDX) microanalysis was performed on TEM using INCA X-Sight (Oxford Instruments).

3. Results and discussion

Silica encapsulation of individually separated nanoparticles is advantageous for bioconjugation and applications to (nano)biotechnology, because silica is nontoxic and easy to functionalize, and protects core nanoparticles from deleterious reactions such as oxidation. Especially in the case of AuNPs, silica encapsulation would be one of the methods for stabilizing AuNPs and making them applicable to (nano)biotechnological areas.

In this work, we biomimetically formed an ultrathin silica layer on AuNPs, resulting in AuNP/silica core/shell hybrids. The procedure used in this paper involves simple two steps: formation of imidazolium ion-presenting SAMs on AuNPs and biomimetic silicification (Scheme 1). The AuNPs were synthesized by the standard chemical reduction method using citrate, and the average diameter of the resulting AuNPs was 17 nm with a standard deviation of 5.6 nm [16]. The formation of imidazolium ion-presenting SAMs was achieved by ligand exchange method. Since the bond strength between Au and sulfur is stronger than that between Au and citrate, citrates could be exchanged with thiol. During the ligand exchange step, we observed the aggregation of AuNPs. However, the incubation of the resulting AuNPs in the acidic solution (10 mM HCl) led to the well dispersion of AuNPs. After the exchange, the result-

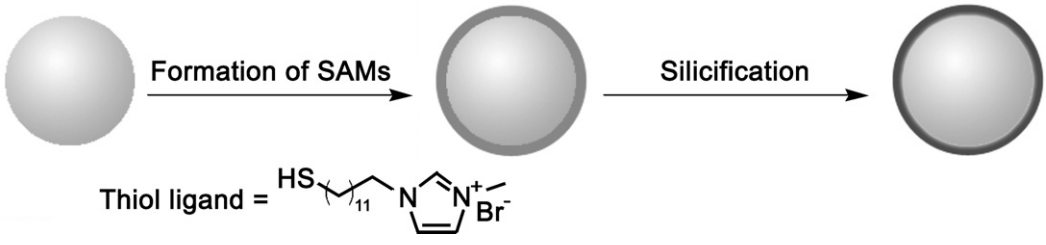

Scheme 1. Schematic description of the procedure.

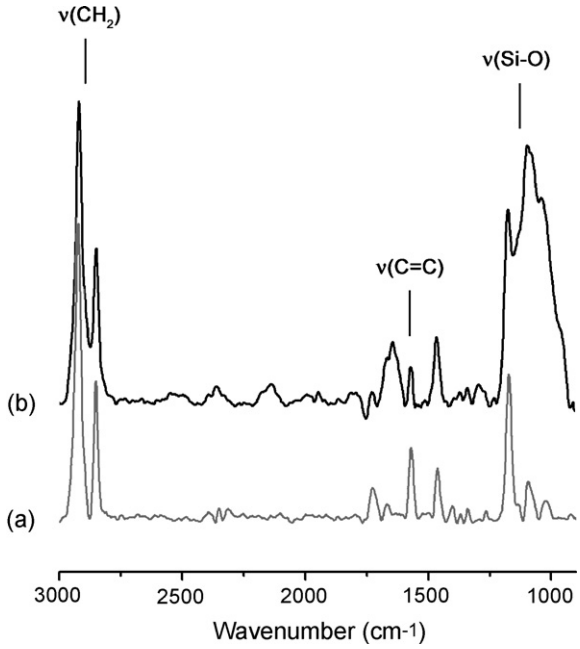

Fig. 1. FT-IR spectra of (a) imidazolium ion-immobilized AuNPs and (b) AuNP/silica hybrids.

ing AuNPs were characterized by IR spectroscopy. We observed the C=C stretching band at 1569 cm^{-1} as well as C–H asymmetric and symmetric stretching bands at 2920 and 2850 cm^{-1} [17], which confirms that the SAM was successfully formed (Fig. 1a) [18]. After washing the AuNPs with water several times, the imidazolium ion-immobilized AuNPs were suspended in an aqueous phosphate buffer (pH 6.0) solution. Silicification was then performed by mixing the nanoparticle solution with an HCl solution (1 mM) of TMOS (100 mM) at room temperature. After stirring for 1 h, the hybrids were washed through centrifuging/resuspending in deionized water.

The formation of the AuNP/silica hybrids was confirmed by FT-IR spectroscopy, TEM, UV–vis spectroscopy, and EDX analysis. In the IR spectrum, the C–H asymmetric and symmetric stretching bands of organic templates at 2920 and 2850 cm^{-1} remained to be observed. In addition to the peaks, the IR spectrum showed new characteristic peaks of silica at 1000–1250 cm^{-1} (Fig. 1b), which were assigned as Si–O antisymmetric stretching [19]. In agreement with the FT-IR spectrum, the EDX data showed a Si peak at 1.74 keV (Fig. 2a). Fig. 2b and c show the TEM micrographs of the hybrids with different magnifications. The average diameter of hybrids was measured to be about 20 nm, which indicated that the thickness of the silica layer was 1.5 nm. The value of 1.5 nm approximately coincided with the thickness of imidazolium ion-presenting SAMs [14].

As shown in Fig. 3, the UV–vis spectra showed a little red shift in the maximum absorption peak of the AuNPs after the SAM formation and the silicification. The peak was shifted from 522.5 to 525 nm after the SAM formation and to 526.5 nm after the silicification, respectively. It is known that the position of the maximum peak is very sensitive to the optical and electronic properties of the medium surrounding the particles

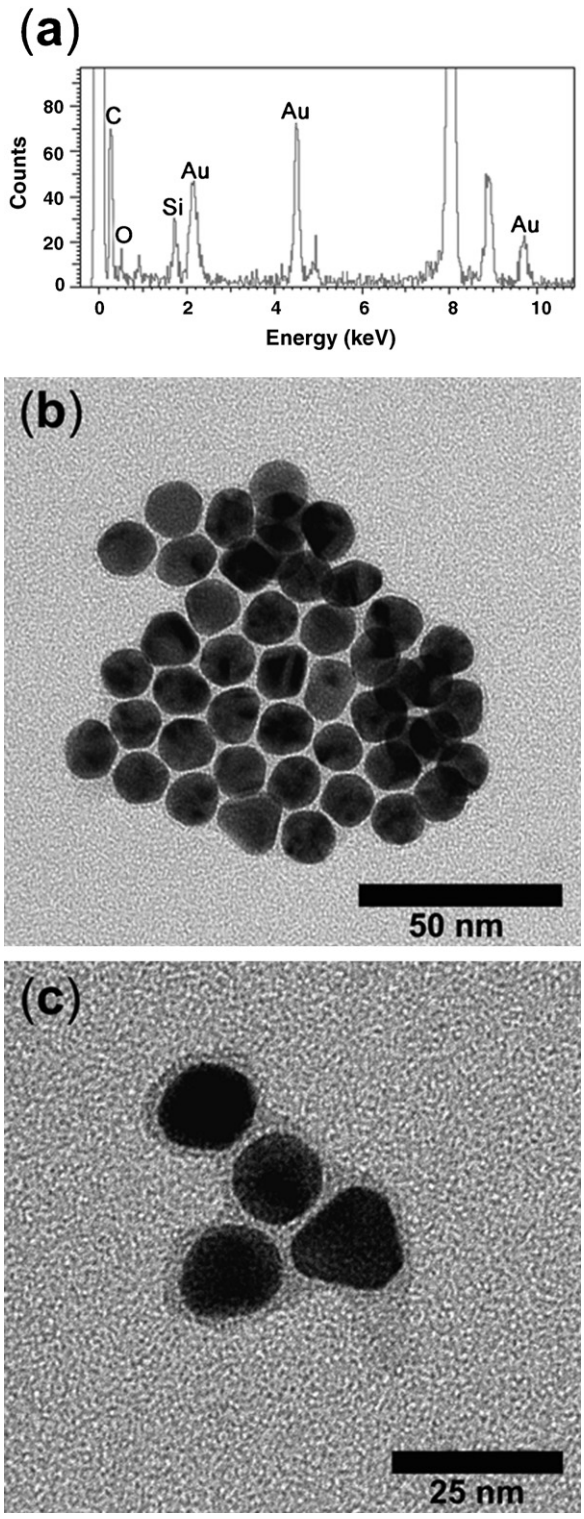

Fig. 2. (a) EDX spectrum of AuNP/silica hybrids and (b) and (c) TEM images of AuNP/silica hybrids.

[20,21]. In both cases of imidazolium ion-immobilized AuNPs and AuNP/silica hybrids, the observed red shift of the plasmon resonance peak may have resulted from changes in the surface dielectric constant of the nanoparticles and the local refractive index around the nanoparticles [12,22–24]. The UV–vis spectra also confirmed that the AuNP/silica hybrids were separated

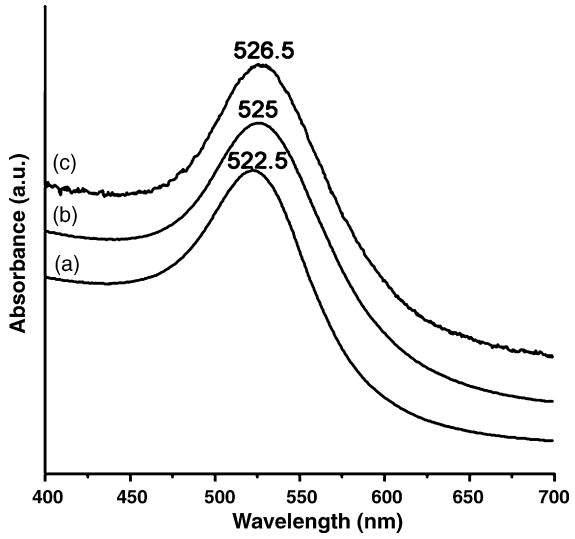

Fig. 3. UV–vis spectra of (a) AuNPs, (b) imidazolium ion-immobilized AuNPs, and (c) AuNP/silica hybrids.

individually, because particle aggregation generally leads to the severe red shift in the maximum absorption peak [17].

4. Conclusion

In this paper, we described a biomimetic approach to the formation of ultrathin (∼1.5 nm) silica-coated AuNPs by using a combination of the formation of SAMs and biosilicification [12]. The method developed in this work is rather simple and does not require any harsh conditions for silica layer formation. We believe that the AuNP/silica hybrids would be useful as a bioprobe or sensor through further surface functionalizations [25], and the synthetic strategy developed in this paper could be applied smoothly to other nanoparticles, such as quantum dots and magnetic nanoparticles, with a proper choice of molecules for SAMs.

Acknowledgments

This work was supported by the National R&D Project for Nano Science and Technology (I.S.C) and Basic Research Program (R01-2006-000-10426-0) from KOSEF (S.-g.L.). FT-IR spectrophotometer was purchased by a research fund from the Center for Molecular Design and Synthesis.

References

[1] F.E. Round, R.M. Crawford, D.G. Mann, The Diatoms: Biology & Morphology of the Genera, Cambridge University Press, Cambridge, UK, 1990.
[2] V.C. Sundar, A.D. Yablon, J.L. Grazul, M. Ilan, J. Aizenberg, Nature 424 (2003) 899.
[3] M. Sumper, Angew. Chem. Int. Ed. 43 (2004) 2251.
[4] M. Sumper, S. Lerenz, E. Brunner, Angew. Chem. Int. Ed. 42 (2003) 5192.
[5] S.V. Patwardhan, N. Mukherjee, S.J.J. Clarson, Inorg. Organomet. Polym. 11 (2001) 193.
[6] E. Brunner, K. Lutz, M. Sumper, Phys. Chem. Chem. Phys. 6 (2004) 854.
[7] M.R. Knecht, D.W. Wright, Langmuir 20 (2004) 4728.
[8] S.V. Patwardhan, S.J. Clarson, Silicon Chem. 1 (2002) 207.
[9] R.K. Iler, The Chemistry of Silica: Solubility, Polymerization, Colloid and Surface Properties, and Biochemistry, Wiley Interscience, New York, 1979.
[10] D.J. Kim, K.-B. Lee, Y.S. Chi, W.-J. Kim, H.-j. Paik, I.S. Choi, Langmuir 20 (2004) 7904.
[11] D.J. Kim, K.-B. Lee, T.G. Lee, H.K. Shon, W.-J. Kim, H.-j. Paik, I.S. Choi, Small 1 (2005) 992.
[12] S.M. Kang, K.-B. Lee, D.J. Kim, I.S. Choi, Nanotechnology 17 (2006) 4719.
[13] W.K. Cho, S.M. Kang, D.J. Kim, S.H. Yang, I.S. Choi, Langmuir 22 (2006) 11208.
[14] B.S. Lee, Y.S. Chi, J.K. Lee, I.S. Choi, C.E. Song, S.K. Namgoong, S.-g. Lee, J. Am. Chem. Soc. 126 (2004) 480.
[15] M.A. Hayat, Colloidal Gold: Principles, Methods, and Applications, Academic press, San Diego, 1989.
[16] D.J. Kim, S.M. Kang, B. Kong, W.-J. Kim, H.-j. Paik, H. Choi, I.S. Choi, Macromol. Chem. Phys. 206 (2005) 1941.
[17] R.G. Snyder, H.L. Strauss, C.A. Elliger, J. Phys. Chem. 86 (1982) 5145.
[18] H. Itoh, K. Naka, Y. Chujo, J. Am. Chem. Soc. 126 (2004) 3026.
[19] K. Moller, T. Bein, R.X. Fisher, Chem. Mater. 7 (1999) 665.
[20] C.F. Bohren, D.F. Huffman, Absorption and Scattering of Light by Small Particles, Wiley, New York, 1983.
[21] U. Kreibig, M. Vollmer, Optical properties of metal clusters Springer Series in Material Science, 25, Springer-Verlag, Berlin, 1995.
[22] P. Mangeney, F. Ferrage, I. Aujard, V. Marchi-Artzner, L. Jullien, O. Ouari, E.D. Rekai, A. Laschewsky, I. Vikholm, J.W. Sadowski, J. Am. Chem. Soc. 124 (2002) 5811.
[23] L.M. Liz-Marzán, M. Giersig, P. Mulvaney, Langmuir 12 (1996) 4329.
[24] F. García-Santamaría, V. Salgueiriño-Maceira, C. López, L.M. Liz-Marzán, Langmuir 18 (2002) 4519.
[25] S. Liu, M. Han, Adv. Funct. Mater. 15 (2005) 961.